Journal of Hazardous Materials 500 (2025) 140424

Contents lists available at ScienceDirect

Journal of Hazardous Materials

journal homepage: www.elsevier.com/locate/jhazmat

Simulated sunlight exposure as a prerequisite for the biodegradation of persistent microplastics

Eva-Maria Teggers [a,b,c,*], Svenja Winterhoff [a], Svetlana Heck [a], Jonas Hardebusch [a], Boris Meisterjahn [a,**], Markus Simon [a], Dieter Hennecke [a], Roman Heumann [b], Holger Egger [d], Philipp Dalkmann [d], Andreas Schäffer [c,1], Annika Jahnke [c,e,1]

[a] Fraunhofer Institute for Molecular Biology and Applied Ecology IME, Auf dem Aberg 1, Schmallenberg 57392, Germany
[b] INVITE GmbH, Otto-Bayer-Straße 32, Cologne 51061, Germany
[c] Institute for Environmental Research, RWTH Aachen University, Worringerweg 1, Aachen 52074, Germany
[d] Bayer AG, Research & Development, Alfred-Nobel-Straße 50, Monheim 40789, Germany
[e] Helmholtz Centre for Environmental Research - UFZ, Department of Exposure Science, Permoserstraße 15, Leipzig 04318, Germany

HIGHLIGHTS

- Photooxidation led to fragmentation and release of ^{14}C-labeled compounds.
- Aminocaproic acid was identified as a photooxidation product of polyurea.
- Simulated sunlight increased polyurea biodegradation in laboratory tests.
- Coupled OECD test methods can reflect potential environmental degradation pathways.
- Radiolabeling allowed precise tracking of polymer mineralization to $^{14}CO_2$.

GRAPHICAL ABSTRACT

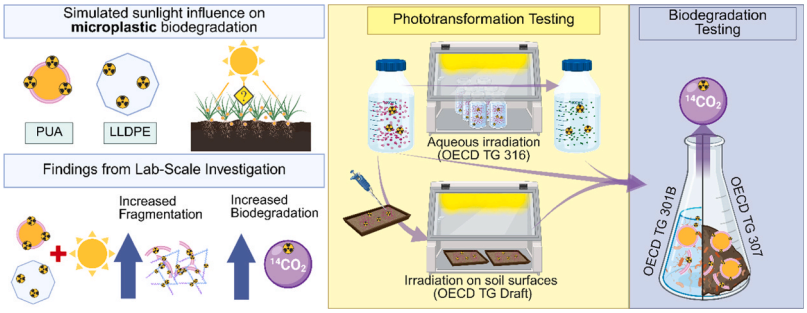

ARTICLE INFO

Keywords:
Microplastics
Photooxidation
Biodegradation
Polyurea microcapsules
Radiolabeling

ABSTRACT

The environmental fate and biodegradability of microplastics (MPs) are key concerns in regulatory and scientific contexts. Standard biodegradation testing effectively evaluate microbial decomposition, but overlook crucial abiotic processes, particularly photooxidation, which may significantly alter polymer structures and their susceptibility to microbial breakdown. Therefore, we investigated how simulated sunlight exposure influences the subsequent (bio)degradability of radiolabeled ^{14}C-polyurea (PUA) microcapsules and ^{14}C-linear low-density polyethylene (LLDPE) particles. Using standardized OECD test guidelines, we conducted coupled photo- and biodegradation experiments in both aqueous and soil environments. Our results demonstrate that simulated sunlight exposure led to fragmentation of PUA microcapsules and the release of low-molecular-weight ^{14}C-labeled compounds, such as aminocaproic acid. Irradiated PUA microcapsules showed significantly enhanced biodegradation in aqueous (up to $28 \pm 4.05\ \%_{AR}$, OECD TG 301B) and soil-based tests (up to $63.2 \pm 13.4\ \%_{AR}$, OECD TG 307), compared to negligible biodegradation in non-irradiated controls. In contrast, LLDPE MPs

* Corresponding author at: Fraunhofer Institute for Molecular Biology and Applied Ecology IME, Auf dem Aberg 1, Schmallenberg 57392, Germany.
** Corresponding author.
E-mail addresses: eva.teggers@rwth-aachen.de (E.-M. Teggers), boris.meisterjahn@ime.fraunhofer.de (B. Meisterjahn).
[1] Andreas Schäffer and Annika Jahnke share the last authorship.

https://doi.org/10.1016/j.jhazmat.2025.140424
Received 4 June 2025; Received in revised form 31 October 2025; Accepted 7 November 2025
Available online 8 November 2025

demonstrated only minor changes. These findings establish that abiotic weathering processes substantially influence MP biodegradability for certain polymer types, and demonstrate the necessity of incorporating realistic environmental exposure conditions into standardized testing protocols. This study improves the understanding of MP degradation pathways and supports more comprehensive regulatory evaluation strategies.

1. Introduction

The extensive production of plastics, including microplastics (MPs), and their uncontrolled emissions into the environment raise major concerns for human and environmental health. While most MP research has focused on aquatic systems, MP pollution in agricultural soils has been less investigated but its relevance is increasingly recognized. A major source of MPs in soil is the fragmentation of plastic mulch films by weathering, including abiotic processes such as sunlight exposure. Primary MPs, intentionally manufactured, also receive attention, with examples including polymer seed coatings and controlled-release fertilizers.

Encapsulated plant protection products (PPPs), represent a lesser-known source of primary MPs. In such products, the active ingredient is enclosed within a polymer microcapsule to enable controlled release and prolonged efficacy. Reports by the Food and Agriculture Organization [26], the United Nations Environment Programme [68], and the Center for International Environmental Law (CIEL, [11]) identify encapsulated pesticides as a potential contributor to MP pollution in soils and related food security risks. In the past, regulatory risk assessments for PPP have considered only the active ingredient, neglecting the fate and potential persistence of the polymeric shell [18,38]. Only recently attention has been given to the full formulation, including polymer-based carriers, as highlighted by Brunning et al. [10] and Nederstigt et al. [48]. The EU Annex XV Restriction Report [22] estimated that capsule suspensions of PPPs account for ~ 500 t of MPs released annually to agricultural soils in Europe.

One example is Prosper 300 CS (Bayer AG), a systemic fungicide contained in polyurea (PUA) microcapsules. Based on product application rates, the estimated worst-case scenario for microplastic (MP) emissions is 150 g/ha per season, assuming a polymer content of 1–5 % and up to three applications. These capsule suspensions are directly applied to agricultural soils, hence their environmental fate, in particular the assessment of their persistence, demands further investigation.

The European Union has recently restricted intentionally added MPs, targeting primary MPs 0.1–5 mm in size added to products such as cosmetics, fertilizers, detergents, and paints. Excluded are soluble, naturally polymerized, non-carbonaceous, and biodegradable primary MPs. For the latter, biodegradability must be demonstrated according to Appendix 15 of Annex XVII to Regulation (EC) No 1907/2006 (REACH, [23]). Current standard methods (OECD, ISO, SI – Table S1) focus on ultimate biodegradability, usually measured as CO_2 evolution, without accounting for abiotic weathering processes such as photooxidation, mechanical stress, hydrolysis, or thermal degradation, even though these can strongly influence MP environmental fate [13,28,46,73].

Recent literature has noted limitations of existing test methods for MPs' biodegradability [12,31,32,47,61,64]. Biodegradability tests were designed for soluble or low-molecular-weight (LMW) chemicals, where defining biodegradation solely by mineralization is reasonable for degradation screening. For polymers and plastics, which may consist of a complex mixture of molecules with varying molecular weights, likely including additives or other plastic-associated compounds, mineralization as only endpoint can misrepresent persistence. Polymeric microcapsules pose additional challenges. Due to their low polymer content and multi-component composition they complicate biodegradation testing, not to mention MP extraction procedures that can bias test results [37]. From a scientific perspective biodegradation of polymers is usually divided into four steps: biodeterioration, depolymerization, bioassimilation, and mineralization [32,43]. Therefore, alterations such as MP fragmentation and the release of plastic-associated compounds and transformation products might be relevant endpoints for degradation testing.

Photooxidation is a primary driver of polymer aging [27,33,41,44], altering surface chemistry and increasing susceptibility to microbial attack. Impurities or sorbed pollutants can accelerate photooxidation or promote indirect photolysis through reactive oxygen species (ROS) formation [21,73]. Dissolved substances such as cations, anions, dissolved organic matter (DOM), and minerals may further modulate these processes [15,19,74,77]. While DOM can act as a photosensitizer [6,45,55,69,75], other constituents may quench ROS, resulting in slower degradation [42,71,72].

Environmental fate comprises multiple processes, yet most studies address them separately (e.g., photochemical or biodegradation). Recent reviews and studies highlight that photooxidation can substantially alter polymer chemistry, size distributions, sorption behavior, and corresponding bio-interactions but understanding its influence on subsequent biodegradation remains largely absent from current testing strategies. This represents not only a scientific knowledge gap but also a regulatory gap in assessing the environmental persistence of MPs under realistic conditions, particularly for microcapsule MPs. The European Food Safety Authority (EFSA) has explicitly cautioned that excluding surface processes such as photolysis from persistence assessments can lead to overestimated degradation half-lives ($DegT_{50}$) and false-positive classifications of substances as persistent [24].

Our study addresses these gaps by investigating whether simulated sunlight exposure impacts the subsequent biodegradability of MPs. Using PUA microcapsules as a representative primary MP and linear low-density polyethylene (LLDPE) as a source for persistent secondary MP, we assessed biodegradation in both aqueous and soil systems subsequent to phototransformation. The study is particularly relevant as it demonstrates a sequential testing strategy combining established regulatory guidelines [52] and an OECD Draft TG [49] for simulated sunlight exposure, OECD TG 301 [50] for screening biodegradation, and OECD TG 307 [51] for biodegradation in soil, linking abiotic weathering to biodegradation outcomes. We used radiolabeled polymers to enable a precise mass balance analysis, mineralization tracking, and identification of transformation products.

2. Material and methods

2.1. Polymers

^{14}C-labeled PUA microcapsules (approx. 3.49 MBq/mg, Bayer AG, Germany) were synthesized in a similar way as described in the patent publication WO2021136758 [39]. The synthesis was performed by the interfacial polymerization of diisocyanate and polyamine in an oil-in-water emulsion. For the radioactive labeling, [1,6-^{14}C] hexamethylenediamine (HMDA, 1887 MBq/mmol, Tjaden Biosciences LLC, USA), together with modified polymeric diphenylmethane diisocyanate (pMDI) were used. The pMDI comprised ≥ 2 binding sites, creating a crosslinked polymer structure. Additional components in the suspension included an organic phase, an oil (8.59 wt% of the undiluted CS, Solvesso 200 ND, ExxonMobil, USA), a dispersant (0.23 wt%, Reax 88, Ingevity Holdings SPRL, USA), and water (90.9 wt%). In a second approach, PUA was synthesized with a modified pMDI additionally containing ester functions in the structure with the intention to increase biodegradability of the final polymer structure (PUA_{mod}). The PUA microcapsules are used for the encapsulation of pesticides and are present

in certain pesticide formulations (e.g., in the fungicide Prosper 300 CS https://www.cropscience.bayer.it/prodotti/fungicidi/prosper-300-cs, Bayer AG) which are currently available on the European market. For the radiolabeled material of this study, both PUA and PUA_{mod} were synthesized on a smaller scale (approx. 200:1 to production scale and approx. 10:1 to normal lab scale), requiring lower concentrations and smaller high-shear equipment (ULTRA TURRAX Tube Disperser, IKA-Werke GmbH & CO. KG, Germany). The polymeric shell amounted to less than 1 wt% of the ^{14}C-suspension (w/w).

The PUA and PUA_{mod} were purified by filtration through a 12 µm pore-sized cellulose nitrate filter (Whatman AE 100, Cytiva, USA) to remove residual non-polymerized ^{14}C-compounds and subsequently resuspended in ultra-high-quality (UHQ) water (PURELAB Ultra, ELGA LabWater, Germany) by ultrasonic bath treatment (Sonorex Super RK514H, Bandelin GmbH & Co. KG, Germany) as described by Teggers et al. [64]. The size distribution of the PUA and PUA_{mod} suspensions was determined using laser diffraction particle size analysis (PSA, Mastersizer 2000, Malvern Panalytical Ltd, UK).

^{14}C-labeled LLDPE MPs (70.46 MBq/g) were synthesized based on methods described by Sinn et al. [62] and Quijada et al. [54], using ^{14}C-1-octadecene (2035 MBq/mmol, American Radiolabeled Chemicals Inc., USA) and cryo-milled in order to imitate MPs originating from agricultural mulch films, and their particle size distribution was analyzed using PSA by Analysette 22 NanoTec, Fritsch GmbH, Germany. For our experiments, the ^{14}C-cellulose was dissolved in 1 N sodium hydroxide (NaOH) and for application, 700 µL NaOH was dissolved in 7.5 mL UHQ water for application with a radioactivity of 10.1 ± 0.07 kBq (average of $n = 4$ and standard deviation (SD)).

2.2. Test soils

Reference soils RefeSol 01-A and 03-G (https://www.refesol.de/, Fraunhofer IME, Schmallenberg, Germany; Supplementary information (SI - Table S2) were utilized for the photodegradation and biodegradation tests. RefeSol 01-A soil consists of a sandy loam with light humic properties and an organic carbon (OC) content of 1.03 %, representative of typical arable soil properties. RefeSol 03-G represents a grassland soil, with a silty loam texture, comprising higher contents of silt, clay and organic carbon (OC: 3.87 %). Both are representative of agricultural areas in Germany and are accepted by the German Federal Environment Agency for use in regulatory guideline studies, e.g., addressing the biodegradation of chemicals. Prior to testing, the soil was sieved to achieve a particle size of ≤ 2 mm, and its water content was adjusted to 50 % of its maximum water holding capacity of 239 g/kg (WHC_{max}, SI – Table S2).

2.3. Quantification of radioactivity in different compartments

Generally, the extent of mineralization as an endpoint of (bio) degradation was calculated based on the evolved $^{14}CO_2$, which was trapped in NaOH in a flow-through system. For the biodegradation test in soil (OECD TG 307) and for the irradiation on soil surfaces (OECD Draft TG), additional absorption traps containing sulfuric acid (H_2SO_4) and ethylene glycol were used to trap volatile alkaline and organic ^{14}C-compounds, respectively. Since we tested ^{14}C-labeled polymers, the aeration of the flow-through setup could be done using ambient air instead of CO_2-free synthetic air. The NaOH traps were sampled every 2–19 days during the incubation period, depending on the current rate of $^{14}CO_2$ development. The first NaOH samples were taken after 2 or 3 d, and subsequent sampling intervals were adjusted based on the radioactivity measured in the previous 2 d. If only a small amount of $^{14}CO_2$ had developed, the next sample was taken after a longer incubation period. Conversely, high levels of detected radioactivity suggested a rapid formation of $^{14}CO_2$. Therefore, sampling was performed in shorter sampling intervals. The radioactivity within the traps was quantified using liquid scintillation counting (LSC). For this purpose and depending on the test medium (alkaline, acidic, organic), 0.5 mL or 1 mL NaOH were combined with 4 mL of the LSC cocktail Picofluor Plus (Perkin Elmer, Germany), 0.5 mL ethylene glycol was combined with 10 mL of the LSC cocktail Supersolve X (Zinsser Analytics, Germany), and 0.5 mL H_2SO_4 was combined with 4 mL of the LSC cocktail Supersolve X and measured with a liquid scintillation counter (HIDEX 600 SL LSC, HIDEX Oy, Finland). The activity in aqueous phases was quantified, e.g., after the end of the OECD TG 301B biodegradation test by combining 1 mL of the sample with 4 mL Supersolve X. The remaining radioactivity in soil, either after irradiation (OECD Draft TG) or upon terminating the biodegradation test (OECD TG 307), was quantified by first drying the soil, where necessary, and then combusting subsamples of approx. 300 mg in an oxidizer (HIDEX 600 OX, HIDEX Oy, Finland). The resulting $^{14}CO_2$ from the combustion was collected in specific LSC-cocktail Oxysolve C-400 (Zinsser Analytic GmbH, Germany) and quantified by LSC-analysis.

2.4. Simulated sunlight irradiation

2.4.1. General irradiation settings

Two different irradiation methods (MI and MII, Fig. 1) were applied to simulate potential, relevant environmental photooxidation to which the pristine polymers might be exposed in order to assess the size distribution after simulated sunlight exposure and the biodegradation. The irradiation was either performed in an aqueous setting following the OECD TG 316 [52] "Phototransformation of Chemicals in Water" (MI) or on soil surfaces (MII) as described in OECD Draft TG [49] "Phototransformation of Chemicals on Soil Surfaces".

All procedures were performed under continuous irradiation in the chamber of a SUNTEST CPS+ device (295–800 nm, Atlas Material Testing Technology GmbH, Germany), equipped with a Xenon lamp of a light intensity of 75 W/m^2 at 300–400 nm according to the manufacturer's specification. The intensity was verified using the BLACK-Comet UV–VIS Spectrometer (BLK-CR2, StellarNet, Inc., USA). The irradiation energy was translated to equivalent days of natural sunlight of summer days in the Northern hemisphere (30–50°N) according to the calculation as described in the OECD Draft TG [49]. Table 1 provides an overview of the exposure durations applied in the respective testing procedures for each irradiation method.

In addition to the air conditioning system of the SUNTEST CPS+, a cryostat using ethylene glycol for cooling the base of the soil surface and the base of the vials was installed (see SI - Fig. S1- E), F)) to maintain a temperature of less than 35 °C in the aqueous suspensions and to cool down the soil surface temperature. The temperature during all irradiation experiments was monitored using thermo data loggers (EL-USB-TP and EL-USB-TP-LCD; accuracy ±0.55 °C), with measurements recorded at hourly intervals. The sensor positions are shown in the SI - Fig. S1, D) and H). For the OECD Draft TG one sensor was placed in the soil surface chamber and one outside the chamber. For the aqueous irradiation the sensor was placed at the bottom of the irradiated Quartz glass vial. After light exposure, the radioactivity of the suspension and of the soil was determined for mass balance analysis.

2.4.2. Aqueous irradiation (MI)

For the aqueous irradiation of the PUA_{mod} (**MI-Procedure 2**, Fig. 1 and Table 2), six replicates of 15 mL PUA_{mod} consisting of an applied radioactivity (AR) of 5.23 ± 0.21 kBq/15 mL were prepared in quartz glass vials (Ø 2.6 cm, 10.5 cm height, SI - Fig. S2) and placed in the irradiation chamber. Three vials were sealed with gas-tight quartz glass lids and used for the downstream biodegradation test (OECD TG 301B) and the remaining three were closed with quartz glass lids, which were equipped with an input and an output that were connected to a flow-through system to trap potentially evolving $^{14}CO_2$ in NaOH (see Section 2.3 for details on the quantification of radioactivity). **MI-Procedure 1** and **MI-Procedure 3** (Fig. 1, Table 2) were performed with a higher AR than 5.23 ± 0.21 kBq/15 mL. Five replicates each containing 15 mL

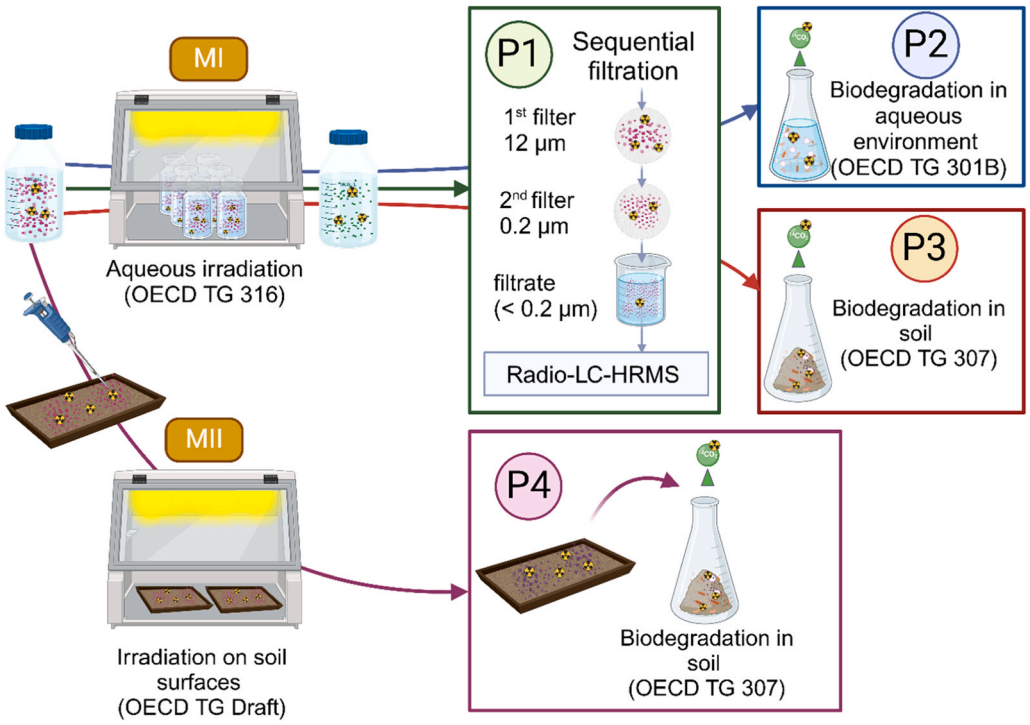

Fig. 1. Procedures (P) to investigate the influence of simulated sunlight exposure of MPs by implementing two different irradiation methods (MI and MII) on the biodegradation and fragmentation of the MPs using coupled standardized guidelines for irradiation and biodegradation tests. Details of the performed procedures are provided in Table 2.

Table 1
Overview of irradiation exposure durations and test materials used in the respective testing procedures.

Procedure	Irradiation Method	Material	Days of Irradiation [d]/eq. summer days[a]
Procedure 1 and 3	MI - Aqueous Irradiation	PUAmod	13.9/41.5
		LLDPE	13.9/41.5
Procedure 2		PUAmod	13.9/41.5
Procedure 4	MII – Irradiation on soil surface	PUAmod	9.9/29.6
		PUA	
		LLDPE	10.1/30.1

[a] Calculated to the equivalent sunlight energy of natural summer days in the Northern hemisphere (30–50°N) acc. to OECD draft TG.

Table 2
Procedures to investigate the influence of light exposure of MP on their biodegradation and fragmentation using coupled standardized OECD guidelines for irradiation and biodegradation tests. (See Fig. 1 for the illustration of the test methods.).

	Procedure description	Irradiation/ biodegradation following	Tested Material
Procedure 1 (P1)	Aqueous irradiation and sequential filtration	OECD TG 316	PUA_{mod}; LLDPE
Procedure 2 (P2)	Aqueous irradiation followed by biodegradation in aqueous environment	OECD TG 316, OECD TG 301B	PUA_{mod}
Procedure 3 (P3)	Aqueous irradiation followed by biodegradation in soil	OECD TG 316, OECD TG 307	PUA_{mod}
Procedure 4(P4)	Irradiation on soil surface followed by biodegradation in soil	OECD TG 316, OECD TG 307	PUA_{mod}; PUA; LLDPE

of the PUA_{mod} suspension (3.5 ± 0.16 kBq/mL) and five replicates of 15 mL of the LLDPE suspension (4.6 ± 1.95 kBq/mL) were placed in the irradiation chamber.

2.4.3. *Irradiation on soil surfaces (MII)*

For **MII-Procedure 4** (Fig. 1, Table 2), the irradiation of the polymers (PUA_{mod}, PUA, Cellulose and PE) on the soil surface, the setup was according to the draft OECD TG "Phototransformation of Chemicals on Soil Surfaces" [51]. In a first step, 10 g_{dw} (dry weight) soil (RefeSol 01-A, see Section 2.2) were suspended in water in order to be cast in quartz glass dishes (18 × 3.5 × 1 cm, SI - Fig. S2). Thereafter, the dishes were placed in a drying cabinet at 35 °C to generate a dry soil layer with a thickness of approx. 2 mm.

For the application 1.5 mL of PUA or PUA_{mod} (31.7 ± 0.06 kBq/1.5 mL PUA; 26.0 ± 0.04 kBq/1.5 mL PUA_{mod}) were applied ($n = 4$ of the dried soil each). Since in previous tests the SD observed for the aqueous application of the LLDPE suspension was high, in this test exact amounts of 1.7, 1.9, 2.1, and 2.8 mg of LLDPE with a determined specific radioactivity of 56.6 kBq/mg were weighted and mixed into the 10 mL water aliquots (equals to a total applied radioactivity (AR) of 96.1, 107, 119, 158 kBq respectively). These aliquots were then used for preparation of the soil suspension used for generating the soil layer. Overall, two replicates (R1 and R2) were irradiated. According to the draft OECD TG, the temperature of the irradiated soil layer shall be kept at 20 ± 2 °C. However, the proposed set-up of the draft OECD TG inevitably generates a temperature gradient, as the lower part of the soil layer is in close proximity to the cooling system, which is set to ≥ 5 °C and the surface of the soil is directly exposed and heated up upon irradiation from the xenon lamp, reaching up to approx. 80 °C (SI – Fig. S3 and S4).

This means that the soil layer is exposed to extreme temperature conditions and the temperature requirement of the guideline cannot fully be maintained [25,35]. Hence, the two remaining replicates were prepared as dark controls in a drying cabinet in which the temperature was set at the highest observed soil temperature (80°C) during irradiation as worst case for possible temperature-induced degradation. This

approach aimed to reliably distinguish between degradation induced by thermal effects from that induced by temperature combined with the photolytic degradation. The light-exposed soil layers were connected to the flow-through system to trap evolving volatile acidic compounds such as $^{14}CO2$, alkaline and organic compounds during irradiation.

2.5. Biodegradation tests

We applied a two-step testing approach in which simulated sunlight exposure, performed according to OECD TG 316 (aqueous medium) or the OECD Draft TG (soil-surface photolysis), was followed by biodegradation testing using OECD TG 301B or TG 307. This sequence reflects a potential realistic environmental pathway for surface-exposed MPs, where sunlight-driven phototransformation can accelerate microbial degradation. The approach aims to align with current regulatory photolysis guidance, including EFSA recommendations for assessing soil phototransformation products [24].

2.5.1. Biodegradation of light-exposed PUAmod microcapsules in the aqueous medium

The biodegradation of aqueous irradiated PUA_{mod} was investigated following OECD TG 301B "CO_2-Evolution Test" (**MI-Procedure 2,** Fig. 1**,** Table 2). As inoculum we applied filtered supernatant of activated sludge instead of bulk sludge, and the test was modified by measuring $^{14}CO_2$ instead of CO_2 for sensitive assignment to the ^{14}C-PUA_{mod} degradation [64]. To monitor the overall degradation performance of the inoculum, the biodegradation of a standard reference substance for ready biodegradability, labeled sodium benzoate form (benzoic acid [ring-^{14}C (U)] sodium salt, 130 mCi/mmol, American Radiolabeled Chemicals Inc., USA), was included in the same test run. The amount of AR was 2.73 ± 0.04 kBq/8.5 mL for PUA_{mod} ($n = 3$) and 58.3 ± 0.18 kBq/8.5 mL for ^{14}C-sodium benzoate ($n = 1$). Table 3 provides an overview of the incubation times of all applied biodegradation tests.

2.5.2. Biodegradation of light-exposed MPs in soil

For **MI-Procedure 3** (Fig. 1, Table 2) and **MII-Procedure 4** (Fig. 1, Table 2) biodegradation tests following the OECD TG 307 "Aerobic and Anaerobic Transformation in Soil" were performed in the dark with sufficient air supply via the flow-through ventilation system at a temperature of 20 ± 2 °C. For **MI-Procedure 3** 0.5 mL (1.75 KBq) of the irradiated PUA_{mod} suspension was applied to 25 g_{dw} of reference soil (01-A and 03-G). For **MII-Procedure 4**, the irradiated ($n = 2$) and non-irradiated ($n = 2$) soil replicate layers applied with PUA_{mod}, PUA, LLDPE was each combined separately for each material, due to their different positions in the irradiation chamber and related possible differences regarding the irradiation intensity or shading effects. Therefore, both replicates were mixed thoroughly to allow homogenous application and the radioactivity of the soil was determined for balancing the mass in the downstream biodegradation test. For application to the biodegradation test (OECD TG 307) after the soil irradiation experiments, 5 g aliquots of the irradiated soil (SI – Table S4) were applied to 50 g untreated biologically active soil (RefeSol 01-A, 10 days preincubated at 22 ± 3 °C) in triplicates each.

Table 3
Overview of the incubation times of the different biodegradation tests.

Procedure	Irradiation method	Biodegradation test	Material	Days of incubation [d]
Procedure 2	MI – Aqueous irradiation	Screening biodegradation (OECD TG 301B)	PUAmod	28
Procedure 3	MI – Aqueous irradiation	Biodegradation in soil (OECD TG 306)	PUAmod	3
Procedure 4	MII – Irradiation on soil surface	Biodegradation in soil (OECD TG 306)	PUAmod PUA LLDPE	20 20 51

2.6. Sequential filtration of the light-exposed MPs suspensions

For **MI-Procedure 1** (Fig. 1, Table 2) the aqueous irradiated and non-irradiated PUA_{mod} and LLDPE were subjected to sequential filtration. For this size distribution analysis, 0.5 mL of the irradiated (1.12 ± 0.01 kBq/0.5 mL PUA_{mod}, 0.63 ± 0.15 kBq/0.5 mL LLDPE) or non-irradiated (1.75 ± 0.08 kBq/0.5 mL, 2.33 ± 0.98 kBq/0.5 mL LLDPE) PUA_{mod} or LLDPE stock solution was diluted in 49.5 mL water and sequentially filtrated by a 12 µm (Cytiva Whatman®, nitrocellulose filter, Z696919) and a 0.2 µm pore-sized filter (Sartorius, cellulose acetate filter, Type 11107) ($n = 3$). The filters were then dried and the remaining radioactivity sorbed and retained to the filter was determined. Furthermore, the radioactivity of the filtrate (< 0.2 µm) was measured (see Section 2.3).

The filtrate of PUA_{mod} (< 0.2 µm) was further analyzed using ultra-high performance liquid chromatography with high resolution mass spectrometry (UHPLC-HRMS, total range of 100–6000 *m/z;* using the Xcalibur Qual Browser (Version 4.0).) coupled to radiodetection (LB509 - YG 75 S6M, Berthold GmbH & Co. KG, Germany) similar to Teggers et al. [64] to examine whether ^{14}C-labeled LMW compounds had been released from the PUA_{mod} shells due to photodegradation. Details of this analysis are given in the SI – Table S5–S7.

2.7. Data analysis

The recovered amounts of radioactivity were calculated as average values with their respective (±) SD of percentage relative to the applied radioactivity ($\%_{AR}$). For all calculations Microsoft Office Professional Plus Excel (2019) was used. Graphpad Prism 6 was employed for the graphical representation and for testing the significance of the difference between the amount of mineralization of irradiated vs. non-irradiated MPs at the end of the biodegradation test (**MII-Procedure 4**) using an unpaired, non-parametric (due to the small number of replicates of $n = 3$) Mann-Whitney test. However, statistical test results should be regarded with caution due to the small number of replicates per treatment and a restricted number of sampling dates within the OECD 301B and 307 tests. This constrained design reduces the statistical power to detect small or moderate differences and can lead to results that appear non-significant even when biological differences exist. The illustration of Fig. 1 and the graphical abstract was created with BioRender.com.

3. Results and discussion

3.1. Analysis of MPs

The PSA of the PUA_{mod} and PUA resulted in a median particle size of 16.5 µm (10th percentile of 2.1 µm and 90th percentile of 37.1 µm; SI – Table S8) and 15.4 µm (10th percentile of 4.8 µm and 90th percentile of 32.7 µm; SI - Table S8) prior purification. The size distribution of the suspension purified by sequential filtration was reevaluated by including a 12 µm cut-off, resulting in a median particle size of 22.9 µm (PUA_{mod},10th percentile of 14.2 µm and 90th percentile of 45.7 µm) and 20.2 µm (PUA,10th percentile of 13.0 µm and 90th percentile of 36.8 µm) (SI - Table S8, SI – Figs. S5 and S6). The LLDPE MPs had a median size of 147 µm (10th percentile of 48.8 µm to 90th percentile of 343 µm, SI - Table S8) after cryo-milling. Microscopic analysis (SI - Fig. S7) provided qualitative data on the PUA microcapsules and LLDPE MPs.

3.2. Simulated sunlight irradiation (MI and MII)

The average temperatures and the irradiation duration, the degree of

mineralization to $^{14}CO_2$ and the total recovery of the different irradiation procedures (**MI** and **MII**) are presented in Table 5. Details, such as the maximum temperatures and the temperature curves during irradiation are shown in the SI – Figs. S3, S4, S8–S10. $^{14}CO_2$ evolving during irradiation of the aqueous PUA_{mod} suspension of **MI-Procedure 2** did not exceed 3.81 ± 1.53 $\%_{AR}$, in which the recovery was 92.2 ± 1.20 $\%_{AR}$ and the average temperature of the aqueous irradiated samples was 3.99 ± 0.77 °C.

The temperatures of the aqueous irradiations in these procedures remained stable at 32.4 ± 1.60 °C, which was notably higher than the temperatures observed in **MI-Procedure 2**. This discrepancy is likely attributable to the positioning of the temperature sensor, which in **MI-Procedures 1** and **3** was positioned centrally and near the upper region of the vial, rather than in contact with the vial wall or base as it might have been the case in **MI-Procedure 2**. A photograph of the sensor setup is provided in SI – Fig. S1-D). Alternatively, if the temperature difference was not solely due to sensor placement, the elevated temperature in **MI-Procedures 1** and **3** relative to **2** could have contributed to increased $^{14}CO_2$ evolution. The total recovery of radioactivity of **MI-Procedures 1** and **3** was 73.4 ± 1.38 $\%_{AR}$, compared to 92.2 ± 1.20 $\%_{AR}$ in **MI-Procedure 2**. This reduction may indicate a greater loss of radioactivity through mineralization. However, as $^{14}CO_2$ was not quantitatively determined in **MI-Procedures 1** and **3**, this interpretation remains speculative.

Due to a failure of the cooling system during irradiation, the aqueous LLDPE suspension (**MI-Procedure 3)** was exposed to higher temperatures reaching an average temperature of 53.0 °C ± 1.3 °C for 6.8 days out of 13.9 days of the exposure period with an overall average temperature of 43.8 ± 10.3 °C (max. temperature of 62.0 °C; SI – Fig. S10). However, LLDPE is considered thermally stable up to approx. 220 °C in the presence of oxygen [3] and therefore the deviation in temperature was not regarded as relevant.

In contrast to the aqueous irradiation of PUA_{mod}, during the exposure on soil surfaces (**MII-Procedure 4**) to simulated sunlight a higher photomineralization to $^{14}CO_2$ was observed, which amounted to 14.6 $\%_{AR}$ (R1) and 8.02 $\%_{AR}$ (R2) for PUA_{mod} and for PUA to 14.11 $\%_{AR}$ (R1) and 1.55 $\%_{AR}$ (R2), respectively (Table 2). The high deviations between both replicates is most likely caused by a leakage of the flow-through system. No other alkaline or organic ^{14}C-volatiles were found in the H_2SO_4 and ethylene glycol traps, respectively. Since the soil layer was dried before light exposure, the formation of $^{14}CO_2$ most likely resulted from abiotic photooxidation reactions rather than biological processes converting the polymer into $^{14}CO_2$. Supporting this finding, 107 ± 9.51 $\%_{AR}$ PUA_{mod} and 104 ± 11.2 $\%_{AR}$ PUA of total AR were recovered from the samples that were kept in darkness, indicating that no radiolabeled volatile compounds evolved without light exposure. Thus, the observed $^{14}CO_2$ formation is attributable to abiotic oxidation and cleavage of the polymer backbone, indicating the occurrence of photo-initiated mineralization. Such abiotic mineralization, though limited in extent, also reflects the degree of chemical functionalization and chain scission that likely influenced the polymers' subsequent particle size changes and biodegradability (see Sections 3.4 and 3.5). Studies of Bhargava et al. [8] and Che et al. [14] investigated the chemical changes of PUA and polyurethane coating by attenuated total reflectance-Fourier transform infrared (ATR–FTIR) spectroscopy after UV-light exposure (0.7522 $W/m^2/nm$) with irradiance at the peak radiation wavelength of 313 nm, tested every 200 h up to 1000 h) and after 150 days exposure in the marine atmosphere, respectively. They found that the absorbance peaks that can be attributed to urea bonds (C-N), carbonyl groups (C═O) and ester bonds (C–O–C) had been decreased after the exposure, which indicated chain scission and cleavage of these bonds. Regarding our findings, it is conceivable that similar cleavages led to the release of $^{14}CO_2$. However, the implementation of more ester bonds as a modification within the PUA (PUA vs. PUA_{mod}, see Section 2.1) had no substantial influence on the fraction that was mineralized to $^{14}CO_2$. Additionally, by implementing the dark controls, which were incubated at higher temperatures, heat-related degradation as the main affecting factor could be excluded, since no radioactivity was lost due to volatilization. The temperature of the dark controls was maintained at 78.0 ± 1.13 °C (SI - Fig. S3), i.e., higher than for the irradiated samples 70.5 ± 1.86 °C (SI – Fig. S3, Table 4).

Regarding the irradiation of LLDPE on soil surfaces, no $^{14}CO_2$ or other ^{14}C-volatiles were detected (Table 4). The recovery was generally low in the dark controls and the irradiated samples of LLDPE with 52.4 ± 21.7 $\%_{AR}$ and 36.9 $\%_{AR}$, respectively, which could not be explained.

3.3. Alterations of size distribution and release of ^{14}C-compounds (MI – Procedure 1)

The results of the sequential filtration (**MI-Procedure 1**, Fig. 2) revealed that the size distribution of the PUA_{mod} suspension was highly altered by the simulated sunlight exposure (Fig. 2) which indicated disintegration of the PUA_{mod} microcapsules. The PUA_{mod} microcapsules that were kept in darkness still showed a retention of 85.3 ± 5.84 $\%_{AR}$ on the 12 μm filter, as expected (Fig. 2). Minor fractions of the dark controls reached the 0.2 μm filter (0.75 ± 0.44 $\%_{AR}$) or the filtrate (< 0.2 μm) (0.48 ± 0.25 $\%_{AR}$, total recovery of 86.5 ± 5.36 $\%_{AR}$). After light exposure, the majority of the applied radioactivity passed the 12 μm and 0.2 μm filters and was hence found in the filtrate (< 0.2 μm) (102 ± 2.43 $\%_{AR}$) with an overall recovery of 106 ± 2.38 $\%_{AR}$ (Fig. 2). Only negligible amounts of labeled particles were retained by the 12 μm (0.89 ± 0.69 $\%_{AR}$) and 0.2 μm (0.59 ± 0.06 $\%_{AR}$) filters, respectively, after irradiation (total recovery of 102 ± 2.46 $\%_{AR}$). The above-mentioned photooxidation reactions (see Section 3.2) that might lead to chain scission and cleavages within the PUA structure had likely led to the disintegration of the microcapsules to sizes smaller than 0.2 μm. Here, the small size (a median particle size of 22.9 μm), the comparably thin PUA_{mod} microcapsules and the exposure in an aqueous medium need to be considered. Du et al. [20] determined the shell thickness of slightly larger PUA microcapsules (approx. 79 μm) to be between 0.4 and 2.5 μm using Scanning Electron Microscopy (SEM). However, shell thickness is not only related to capsule size, but also influenced by the number of monomers used during microcapsule synthesis. Nonetheless, transferring these findings to our experiments, a much higher proportion of the PUA microcapsules was likely to be exposed to the simulated sunlight than for the bulk polymer LLDPE, and PUA was thus likely more affected than the thicker and mono-constituent LLDPE polymeric particles.

Accordingly, reduced effect was observed for the LLDPE particles that were exposed to simulated sunlight (Fig. 2). Prior to irradiation, the vast majority of the recovered LLDPE particles (total recovery of 57.6 ± 24.1 $\%_{AR}$) were retained by the 12 μm filter 55.1 ± 24.07 $\%_{AR}$ opposed to the second filter (0.2 μm, 1.52 ± 0.31 $\%_{AR}$) or the filtrate (< 0.2 μm, 0.94 ± 0.97 $\%_{AR}$). After light exposure, only 28.2 ± 7.13 $\%_{AR}$ remained on the first filter (12 μm) and 4.79 ± 2.79 $\%_{AR}$ was recovered from the second filter (0.2 μm). When interpreting these results, it has to be kept in mind that the overall recovered radioactivity of this analysis was low and some of the detected amounts differed considerably. Nevertheless, the sequential filtration indicated that LLDPE had partially disintegrated to smaller ^{14}C-compounds or ^{14}C-particles that were released upon simulated sunlight exposure, as a higher amount was recovered in the filtrate (< 0.2 μm, 20.5 ± 1.97 $\%_{AR}$, total recovery 53.5 ± 8.36 $\%_{AR}$) (Fig. 2) upon simulated sunlight irradiation.

A review of Grause et al. [29] summarized the changes of polyolefins due to weathering, especially regarding the exposure to UV irradiation in the presence of oxygen. Even though some polymers such as PE are light-transmitting (transparent), they inevitably include certain fractions of chromophore compounds (e.g., carbonyl functionalities or chain unsaturation), which are formed during production and thermooxidation (e.g., during processing, [1,9,40,56,59]) that can induce photodegradation. Focusing on LLDPE, the initial production of hydroperoxides plays a major role, inducing reactions that may liberate

Table 4
Overview of the different irradiation procedures. Shown are the average irradiation temperature, the mineralization to $^{14}CO_2$ during irradiation and the total recovery for mass balancing both in the percentage of applied radioactivity [$\%_{AR}$].

Irradiation Procedure	Average irradiation temperature [°C]		Minerali-zation to $^{14}CO_2$ [$\%_{AR}$]	Total recovery [$\%_{AR}$]	
	Dark	Irradiation	Irradiation	Dark	Irradiation
Procedures 1 and 3					
PUA_{mod}	-	32.4 ± 1.60	-	-	73.4 ± 1.38
LLDPE	-	43.8 ± 10.3	-	-	54.1 ± 12.5
Procedure 2					
PUA_{mod}	20.8 ± 1.66	3.99 ± 0.77	3.81 ± 1.53	85.1 ± 4.36	92.2 ± 1.20
Procedure 4					
PUA_{mod}	78.0 ± 1.13	70.5 ± 1.86	11.3 ± 4.63	107 ± 9.51	100
PUA			7.83 ± 8.88	104 ± 11.2	94.7
LLDPE	77.3 ± 0.77	69.3 ± 3.39	0.31 ± 0.22	52.4 ± 21.7	36.9

*The irradiation was performed with 75 W/m^2 within of a wavelength range of 300–400 nm (see details in SI – Table S3).

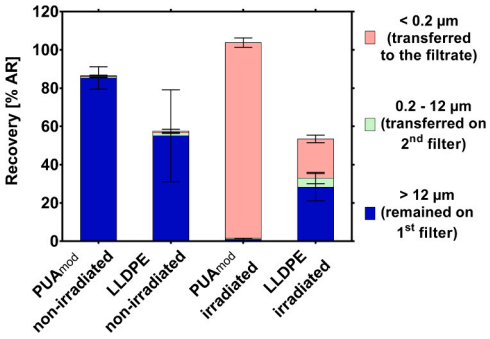

Fig. 2. Proportion of applied radioactivity (AR) recovered in the different fractions obtained by sequential filtration. Displayed are the $\%_{AR}$ of the irradiated and non-irradiated PUA_{mod} and LLDPE suspensions, which was quantified on the first (12 µm pore size) and the second filter (0.2 µm) and in the filtrate (< 0.2 µm).

LMW compounds including carboxylic acid, alcohols and to a lower extent esters [30,67]. Possibly, the liberation of such LMW ^{14}C-compounds resulted in the increased radioactivity in the filtrate (< 0.2 µm) after light exposure.

Andrady et al. [2] found that oxidation reactions were limited to a thin surface layer of the LLDPE of approx. 600 µm. Since the LLDPE in this study had a median size of 147 µm (SI – Table S8) it is likely that the LLDPE particles were completely penetrated by the irradiation and partly fragmented. Supporting this, findings from Pfohl et al. [53] showed that photooxidation in the presence of water increased the fragmentation of LDPE particles under UV aging. In addition, considering that irradiation in an aqueous medium can penetrate from all directions, the distance required to reach the center may be only half the total diameter for spherical particles.

The UHPLC-HRMS analysis of the filtrate (< 0.2 µm) of PUA_{mod} revealed the release of ^{14}C LMW compounds as a result of the light-induced disintegration, which is detailed in SI – Text S2. The radio chromatogram showed one peak (SI – Fig. S11-E)), corresponding to labeled and non-labeled aminocaproic acid (SI – Fig. S11-A), B), C)). By analyzing pure (≥ 99 %) aminocaproic acid as a reference compound (10 ng/mL, Sigma-Aldrich Chemie GmbH, Germany) and a mixture of the reference compound together with the PUA_{mod} filtrate (SI – Fig. S11-D), SI – Fig. S12-D)), the presence of aminocaproic acid was proven. Furthermore, the isotopic pattern analysis (SI – Fig. S13, SI - Text S2) substantiated these findings. ^{14}C-aminocaproic acid is similar to the ^{14}C-labeled monomer ^{14}C-hexamethylenediamine (^{14}C-HMDA) used for synthesis, except that it contains a carboxyl instead of an amine group.

Most likely, the PUA bonds were partially broken by formed radicals and photooxidation processes. Due to formed hydroxyl radicals (•OH) and superoxide anions ($O_2^{\bullet-}$) apparently HDMA was oxidized to produce aminocaproic acid. Oxidative processes were also shown by Si et al. [60], where deamination of primary amines (-NH_2) was induced by radicals. By means of a column recovery test, the eluted radioactivity within the retention time of ($^{14}C_{(2)}$-) aminocaproic acid was quantified and represented 48.5 ± 1.16 $\%_{AR}$ (SI – Fig. S14, recovery of 93.2 ± 1.93 %) of the injected radioactivity. This observation indicates that a large portion of ^{14}C-labeled molecules or oligomers introduced to this analysis can likely be attributed to the elution of ^{14}C-aminocaproic acid.

According to ECHA data (https://echa.europa.eu/es/registration-dossier/-/registered-dossier/22890/5/3/2), aminocaproic acid is readily biodegradable, non-toxic to aquatic organisms and not bioaccumulative suggesting a low environmental concern. Overall, the identification of specific degradation products remains analytically challenging, particularly when dealing with complex polymeric matrices and trace-level compounds. From an environmental perspective, it is important to investigate whether transformation products may form due to environmental exposure conditions that could alter the risk profile of the material. In this case, release of a non-persistent and biodegradable compound was identified. However, other types of polymers and their associated additives may generate different transformation products upon exposure to sunlight, which is a growing concern highlighted in a recent assessment supported by the UNEP but remains largely underexplored [36]. For example, the degradation of side-chain fluorinated polymers has been shown to release perfluorinated substances, including perfluorooctanoic acid (PFOA), over decades under environmental conditions such as those found in soil and water [70]. This observation highlights the importance of investigating whether polymeric materials might release environmentally persistent or toxic transformation products following abiotic processes like light exposure.

In this context, it is important to note that the polymeric shell included not only the radiolabeled HMDA monomer but also co-polymerized isocyanates. As the radiolabel was incorporated into one specific monomer, the assessment of mineralization and degradation pathways was limited to fragments containing that labeled unit. Consequently, the behavior and fate of degradation products derived from non-labeled portions of the polymer were beyond the scope of this study. For a comprehensive understanding of the degradation processes, experiments with isotope labels at other positions of the molecules would be required.

3.4. Biodegradation of light-exposed PUA_{mod} microcapsules in the aqueous medium (MI – Procedure 2)

The results of **MI-Procedure 2**, the aqueous irradiation (Fig. 1) of PUA_{mod} with the downstream biodegradation test resulted in a biodegradation of 28.0 ± 4.05 $\%_{AR}$ in the irradiated suspension. The test outcome is significantly higher than the $^{14}CO_2$ evolution observed in a previous OECD TG 301B study with non-irradiated PUA_{mod} reaching

0.81 $\%_{AR}$ ([64], p = .0303; irradiated vs. non-irradiated PUA_{mod}, test of significance by an unpaired, non-parametric Mann-Whitney test; significant difference indicated by $p < 0.05$) demonstrates that simulated sunlight exposure significantly increased biodegradation. It is likely that the partial biodegradation of the irradiated PUA_{mod} suspension observed in this experiment originated from the mineralization of the released ^{14}C-aminocaproic acid. This interpretation is supported by its safety data sheet's information stating that aminocaproic acid is classified as readily degradable, determined in an OECD TG 301D test with 76 % biodegradation within 28 days of incubation.

3.5. Biodegradation of light-exposed MPs in soil (MI – Procedure 3 and MII – Procedure 4)

With regard to **MI-Procedure 3**, the PUA_{mod} suspension was irradiated in an aqueous environment (see 2.4.2) and subsequently applied to the biodegradation test in soil. Biodegradation of the irradiated PUA_{mod} applying this procedure $^{14}CO_2$ formation amounted to 63.2 ± 13.4 $\%_{AR}$ (RefeSol 01-A) and 62.3 ± 9.65 $\%_{AR}$ (RefeSol 03-G) in the reference soil RefeSol 01-A within 72 h (Fig. 3, right panel). In a parallel study, significant losses were observed for the extraction recoveries of irradiated PUA_{mod} applied to soil [65]. This observation might be attributable to the fast biodegradation of the PUA_{mod}. Therefore, the results of this study may also be relevant for studies investigating extraction methods of aged polymers or plastics. Compared to the biodegradation test results of the irradiated PUA_{mod} in the aqueous setting the CO_2-evolution of the microcapsules irradiated on soil surfaces (**MII-Procedure 4**) reached only 13.6 ± 1.44 $\%_{AR}$ (PUA) and 11.8 ± 3.64 $\%_{AR}$ (PUA_{mod}) (Fig. 3) during 20 days of incubation in soil. The microcapsules of the dark controls showed a negligible biodegradation of 2.52 ± 0.96 $\%_{AR}$ (PUA) and 1.52 ± 0.29 $\%_{AR}$ (PUA_{mod}) (Fig. 3). In this case, irradiation on dry soil likely led to reduced phototransformation due to microcapsule aggregation and adsorption onto the soil surface, which may have caused shading effects and limited light penetration compared with irradiation in water. Consequently, the extent of biodegradation in soil was presumably lower.

The testing in **MI-Procedures 1–3** focused on PUA_{mod} microcapsules, whereas in **MII-Procedure 4** we additionally tested regular, non-modified PUA and LLDPE. PUA modification did not alter biodegradability since both materials were mineralized to similar degrees (p= 0.8 irradiated; p = 0.6 non-irradiated, test of significance by an unpaired, non-parametric Mann-Whitney test; significant difference indicated by $p < 0.05$). Table 5 shows the amounts of mineralization.

The biodegradation of LLDPE MPs was slightly enhanced after their irradiation on the soil surface compared to the non-irradiated dark controls (1.99 ± 0.18 $\%_{AR}$ vs. 0.75 ± 0.14 $\%_{AR}$, respectively, Table 5). The recovery of the biodegradation test in soil for all tested samples was above 80 %, but with a higher variability (elevated standard deviation) for some LLDPE dark controls (see Table 5). Overall, the differences observed between irradiated and non-irradiated PUA and PUA_{mod} samples in the degree of mineralization in the soil biodegradation test indicate a statistical trend ($p < 0.10$, Table 5) toward increased mineralization following simulated light exposure on a soil surface. For LLDPE particles, however, the increase in biodegradation after irradiation, although statistically significant, was minimal and practically not measurable, indicating negligible biological relevance.

3.6. Overall discussion

Our results demonstrate that phototransformation can be a decisive unlocking step in the biodegradation of certain MPs. With regard to PUA microcapsules, simulated sunlight caused near-complete disintegration (~ 98 % of recovered radioactivity in < 0.2 µm size fraction) and the release of a readily biodegradable LMW compound, ^{14}C-aminocaproic acid. These abiotic processes were closely associated with a 28 % mineralization in aqueous OECD 301B tests and > 60 % mineralization in soil OECD 307 tests following aqueous irradiation. Compared with irradiation in water, irradiation on a dry soil surface likely reduced phototransformation due to particle aggregation and surface adsorption, causing shading effects and limiting light penetration, which in turn constrained biodegradation. In contrast, LLDPE particles fragmented to ~ 20.5 $\%_{AR}$ in submicron fractions (< 0.2 µm) after simulated sunlight exposure in an aqueous medium. The increase after soil surface irradiation in mineralization from approximately ~ 1 $\%_{AR}$ to ~ 2 $\%_{AR}$ biodegradation in soil after soil surface irradiation was statistically significant. However, this change represents a rather negligible increase that is not practically measurable, consistent with the chemical resistance of LLDPE to oxidative functionalization [13,28]. These quantified differences confirm that fragmentation alone does not ensure biodegradability; the production of bioavailable transformation products is essential. The results are consistent with the conceptual framework of stepwise polymer degradation (biodeterioration/fragmentation →depolymerization→assimilation→mineralization) and provide regulatory-relevant quantification of each step for two contrasting polymer types.

By applying sequential testing (OECD TG 316 or OECD draft soil-surface photolysis → OECD TG 301B/307), we translated the conceptual link between abiotic and biotic processes into an easily applicable

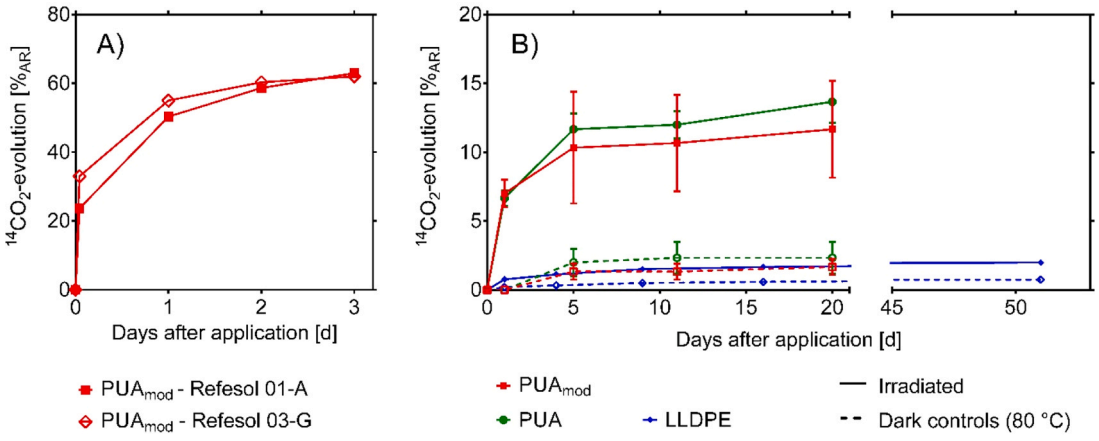

Fig. 3. A) Biodegradation of irradiated PUA_{mod} microcapsules in soil (Refesol 01-A and Refesol 03-G) after irradiation in the aqueous setting (**MI-Procedure 3**). B) Biodegradation of PUA microcapsules with/without ester-bond modification (PUA vs. PUA_{mod}) and LLDPE MPs in soil (Refesol 01-A) after simulated sunlight irradiation or in dark controls incubated at 80 °C on soil surfaces (**MII-Procedure 4**). The biodegradation is plotted as the cumulative portion of applied radioactivity (AR) mineralized to $^{14}CO_2$ relative to the incubation time (average and SD of $n = 3$).

Table 5
Mineralization and recovery of the biodegradation test in soil (OECD TG 307). Test of significance using an unpaired, non-parametric Mann-Whitney test to compare irradiated vs. non-irradiated materials.

MP Material	Mineralization Dark controls [$\%_{AR}$]	Mineralization Irradiated [$\%_{AR}$]	Days of incubation [d]	Significance of difference: irradiated vs. non-irradiated p	Recovery Dark controls [$\%_{AR}$]	Recovery Irradiated [$\%_{AR}$]
PUA_{mod}	1.52 ± 0.29	11.8 ± 3.64	20	0.0873	83.0 ± 8.12	82.0 ± 6.46
PUA	2.52 ± 0.96	13.6 ± 1.44	20	0.0873	122 ± 20.8	109 ± 2.74
LLDPE	0.75 ± 0.14	1.99 ± 0.18	51	* 0.0204	107 ± 37.5	84.0 ± 10.8

* Test of significance by an unpaired, non-parametric Mann-Whitney test; significant difference indicated by $p < 0.05$.

standardized testing approach. While earlier studies have documented photo-oxidative effects on polymers, they rarely quantify both structural changes and mineralization within a regulatory testing framework. Our results show that the influence of phototransformation on subsequent biodegradation is both polymer- and medium-dependent, which becomes apparent only when these processes are examined in sequence. This sequential approach, grounded in established guidelines, reveals mechanistic and regulatorily relevant information that single tests cannot capture.

Previous research has repeatedly suggested that abiotic weathering, particularly photooxidation, can facilitate microbial degradation of plastics, yet direct linkage between observed structural changes and measured ultimate biodegradation (mineralization) within a regulatory testing framework remains rare. For example, Gewert et al. [28] reviewed degradation pathways for marine plastics and highlighted UV- or photooxidation as a prerequisite for microbial colonization. Several studies have confirmed this facilitation effect and have shown that UV- or light-weathering pre-treatments can accelerate fragmentation and promote microbial colonization and breakdown of plastics [7,58,76]. CO_2 evolution measurements in various studies have demonstrated that prior phototransformation can enhance the biodegradability of certain polymers: Rose et al. [57], used the American Society for Testing and Materials (ASTM) D5208 standard "Practice for Fluorescent Ultraviolet (UV) Exposure of Photodegradable Plastics" [5] to UV-aged LDPE and oxo-LDPE prior to aqueous CO_2-respirometry tests. Tantawi et al. [63] applied simulated sunlight in combination with marine biodegradation assays following ASTM D6691-17 [4] "Standard Test Method for Determining Aerobic Biodegradation of Plastic Materials in the Marine Environment by a Defined Microbial Consortium or Natural Sea Water Inoculum" and ISO 23977-1 "*Plastics - Determination of the Aerobic Biodegradation of Plastics Exposed to Seawater - Part 1: Method by Analysis of Released Carbon Dioxide*.". Chen et al. [16] photoaged MPs before degradation was studied in soil microcosms. However, CO_2-based biodegradation studies that support the principle that abiotic processes can facilitate biotic degradation have been rarely conducted. Our work extends this concept by applying a regulatorily relevant sequential testing strategy aligned with OECD guidelines, directly addressing contexts such as the EU MPs restriction and ongoing initiatives to extend REACH provisions to cover polymers. This sequential design bridges observed photooxidative changes to quantifiable biodegradation endpoints in a format suitable for regulatory assessment, enabling interpretation within emerging regulatory frameworks. In contrast to earlier research, we focused on MPs, including PUA microcapsules used for application of PPPs, a formulation type whose environmental fate remains largely unexplored.

PUA microcapsules, such as those in Prosper 300 CS, are applied at relatively low amounts, with a maximum of 150 g/ha permitted per season. In our tests, aqueous irradiation produced high biodegradation (OECD TG 301B with 28 $\%_{AR}$ and ~ 62–63 $\%_{AR}$ in OECD TG 307 in soil), whereas soil-surface irradiation yielded much lower mineralization (12–13.5 $\%_{AR,}$ in OECD TG 307), underscoring the influence of the investigated medium and corresponding light penetration. LLDPE mulch films, applied at ~ 180 kg/ha per season [26], are partially recovered post-use (75–95 %, Hann et al. [34]) but can release persistent residues. In our experiments, even after fragmentation, LLDPE mineralization remained negligible. Such polymer-specific responses indicate that persistence assessments based solely on inherent chemical structure may misrepresent the actual environmental fate.

However, extrapolation of these laboratory results to real environmental conditions must be made with caution. In agricultural contexts, such as the application on plant leaves of PUA-based pesticide formulations like Prosper 300 CS, microcapsules may indeed be exposed to sunlight initially, before potentially being incorporated in the soil. If applied directly to the soil, their exposure to sunlight will probably be minor, compared to the lab experiment, since the MPs might be incorporated to deeper soil layers through irrigation, bioturbation or plowing. According to Tester and Morris [66], physiologically and ecologically relevant amounts of light rarely penetrate more than 4–5 mm into the soil, and Ciani et al. [17] measured that the light penetration depths for soils are in the range of 17–110 μm at 275 nm and 120–300 μm at 700 nm, respectively. Nonetheless, our controlled results illustrate the mechanistic potential for sunlight to alter environmental persistence and highlight conditions under which this process is relevant.

3.7. Regulatory gaps and recommendations

Biodegradability tests according to OECD (e.g. TG 301, TG 307) or ISO guidelines determine whether a chemical is subject to microbial metabolism. These tests were designed for soluble substances for which mineralization is a meaningful endpoint. However, the approach cannot be directly transferred to insoluble polymers, and thus to microplastic particles. For these materials, bioavailability can be constrained by particle size, morphology, and surface chemistry, meaning that mineralization endpoints may underestimate the degradation potential, especially if relevant abiotic transformation processes are not considered. The linkage between abiotic weathering processes, such as photooxidation, and subsequent biodegradation is largely disregarded in current testing strategies, representing a critical scientific and regulatory gap. This combined degradation is particularly relevant for agricultural polymer-based microcapsules or carrier materials, which may undergo structural changes under environmental conditions that may alter their fate. Relying solely on mineralization as an endpoint risks overlooking partial degradation steps or transformations that could be captured by polymer-specific analyses, such as particle size distribution, molecular weight changes, surface analysis and chemical functional group analysis.

Our findings show that for the tested crosslinked PUA MPs, which are classified as persistent, simulated sunlight can be a prerequisite for measurable biodegradation in standard tests. Where there is evidence of environmentally relevant light exposure for a given MP application (to be established by future studies under field conditions), the influence of simulated sunlight (e.g., TG 316 or draft soil-surface photolysis at a defined equivalent sunlight dose) on subsequent biodegradation testing (TG 301/307) should be considered. Ideally, such assessments should report both primary degradation metrics (fragmentation, low-molecular-weight product release) and ultimate mineralization, supported by a mass balance where feasible. This integrated approach

would align regulatory testing with realistic environmental exposure scenarios and reduce the risk of false persistence classifications.

4. Conclusions

The results of this study are not only relevant scientifically, but also from a regulatory perspective. They underscore the need for more comprehensive and realistic assessments of the fate of MPs, particularly by the inclusion of sunlight irradiation as a key abiotic degradation mechanism. By coupling existing standardized guidelines for abiotic and biological degradation, we demonstrated that photooxidation substantially influenced the environmental fate and biodegradability of MPs. Furthermore, our findings highlight that changes in particle size distribution and the formation of phototransformation products, in our case aminocaproic acid, can critically affect the outcome of biodegradation tests. We therefore recommend including such physicochemical characterization in future assessments of the fate of MPs. The use of radiolabeling in the applied tests was crucial for distinguishing $^{14}CO_2$ derived from polymer (bio)degradation from the CO_2 originating from other components in the tested sample. Moreover, the ability to perform precise mass balances based on total recovered radioactivity served as a reliable tool for validating the experimental outcomes. Overall, this study extends the understanding of the environmental fate of MPs, but should be expanded to include related studies under real field conditions.

Environmental Implication

This study demonstrates that abiotic processes, particularly simulated sunlight exposure, can be a prerequisite for the biodegradation of persistent microplastics, such as polyurea (PUA) microcapsules. The results show that phototransformation substantially alters polymer structure, and can lead to increased microbial mineralization in standard laboratory tests. These findings indicate that photodegradation can critically influence polymer fate. Including realistic environmental exposure processes may support more comprehensive assessments of microplastic biodegradation.

CRediT authorship contribution statement

Holger Egger: Writing – review & editing, Supervision, Project administration, Funding acquisition. **Roman Heumann:** Writing – review & editing, Supervision, Project administration, Funding acquisition. **Dieter Hennecke:** Writing – review & editing, Supervision, Project administration, Funding acquisition. **Markus Simon:** Writing – review & editing, Supervision, Project administration, Funding acquisition. **Boris Meisterjahn:** Writing – review & editing, Supervision, Project administration, Funding acquisition. **Jonas Hardebusch:** Methodology, Investigation. **Svetlana Heck:** Investigation, Formal analysis, Data curation. **Svenja Winterhoff:** Investigation, Formal analysis, Data curation. **Eva-Maria Teggers:** Writing – original draft, Visualization, Software, Methodology, Investigation, Formal analysis, Data curation, Conceptualization. **Annika Jahnke:** Writing – review & editing, Supervision. **Andreas Schäffer:** Writing – review & editing, Supervision, Project administration, Funding acquisition. **Philipp Dalkmann:** Writing – review & editing, Supervision, Project administration, Funding acquisition.

Declaration of Generative AI and AI-assisted technologies in the writing process

During the preparation of this work the authors used ChatGPT 4o and 5 Pro and Perplexity Pro (Version August, 2025) for rephrasing and shortening of self-written text. After using this tool/service, the authors reviewed and edited the content as needed and take full responsibility for the content of the publication.

Funding sources

This project was funded by Bayer AG, Crop Science Division. Open Access funding enabled and organized by Projekt DEAL.

Declaration of Competing Interest

The authors declare the following financial interests/personal relationships which may be considered as potential competing interests: Eva-Maria Teggers, Jonas Hardebusch, Boris Meisterjahn, Dieter Hennecke, Markus Simon, Philipp Dalkmann, Holger Egger, Roman Heumann reports financial support was provided by Bayer AG. Philipp Dalkmann, Holger Egger, Roman Heumann, Eva-Maria Teggers reports a relationship with Bayer AG and INVITE GmbH that includes: employment. Holger Egger has patent #WO2021136758 Aqueous Capsule Suspension Concentrates Based on Polyurea Shell Material Containing Polyfunctional Aminocarboxylic Esters licensed to Bayer AG. Philipp Dalkmann and Holger Egger are employees of the Bayer AG Division Crop Science, a leading manufacturer of agricultural chemicals. Roman Heumann and Eva-Maria Teggers are or were employed at INVITE GmbH, Germany, during the investigation time. INVITE GmbH is a cross-industry company with with 50 % business shares belonging to Bayer AG and 50 % business shares belonging to universities (Technical University of Dortmund, Germany and Heinrich Heine University Düsseldorf, Germany). If there are other authors, they declare that they have no known competing financial interests or personal relationships that could have appeared to influence the work reported in this paper.

Acknowledgements

The authors gratefully acknowledge the technical support provided by the team at Fraunhofer IME. In particular, we thank Thomas Hennecke, Christoph Eggenstein-Deimel, and Joana Bräutigam for their valuable advice regarding the experimental work.

Appendix A. Supporting information

Supplementary data associated with this article can be found in the online version at doi:10.1016/j.jhazmat.2025.140424.

Data availability

Data will be made available on request.

References

[1] Allen, N.S., 1986. Recent advances in the photo-oxidation and stabilization of polymers. Chem Soc Rev 15, 373–404.
[2] Andrady, A.L., Lavender Law, K., Donohue, J., Koongolla, B., 2022. Accelerated degradation of low-density polyethylene in air and in sea water. Sci Total Environ 811, 151368. https://doi.org/10.1016/j.scitotenv.2021.151368.
[3] Aniśko, J., Sałasińska, K., Barczewski, M., 2023. Study on thermal stability and degradation kinetics of bio-based low-density polyethylene. Aniśko Polimery 68, 451–460. https://doi.org/10.14314/polimery.2023.9.1.
[4] ASTM. D6691-17 – test method for determining aerobic biodegradation of plastic materials in the marine environment by a defined microbial consortium or natural sea water inoculum; n.d. ⟨https://doi.org/10.1520/D6691-17⟩.
[5] ASTM. D5208 – practice for fluorescent ultraviolet (UV) exposure of photodegradable plastics; 2022. ⟨https://doi.org/10.1520/D5208-14R22⟩.
[6] Bai, Y., Zhou, Y., Che, X., Li, C., Cui, Z., Su, R., et al., 2021. Indirect photodegradation of sulfadiazine in the presence of DOM: effects of DOM components and main seawater constituents. Environ Pollut 268, 115689. https://doi.org/10.1016/j.envpol.2020.115689.
[7] Bao, R., Cheng, Z., Hou, Y., Xie, C., Pu, J., Peng, L., et al., 2022. Secondary microplastics formation and colonized microorganisms on the surface of conventional and degradable plastic granules during long-term UV aging in various environmental media. J Hazard Mater 439, 129686. https://doi.org/10.1016/j.jhazmat.2022.129686.
[8] Bhargava, S., Kubota, M., Lewis, R.D., Advani, S.G., Prasad, A.K., Deitzel, J.M., 2015. Ultraviolet, water, and thermal aging studies of a waterborne polyurethane elastomer-based high reflectivity coating. Prog Org Coat 79, 75–82. https://doi.org/10.1016/j.porgcoat.2014.11.005.

[9] Bracco, P., Costa, L., Luda, M.P., Billingham, N., 2018. A review of experimental studies of the role of free-radicals in polyethylene oxidation. Polym Degrad Stab 155, 67–83. https://doi.org/10.1016/j.polymdegradstab.2018.07.011.
[10] Brunning, H., Sallach, J.B., Zanchi, V., Price, O., Boxall, A., 2022. Toward a framework for environmental fate and exposure assessment of polymers. Environ Toxicol Chem 41, 515–540. https://doi.org/10.1002/etc.5272.
[11] Carlini, G., Drugmand, D., 2022. Sowing a plastic planet: how microplastics in agrochemicals are affecting our soils, our food, and our future. Center for International Environmental Law.
[12] Carmichael, N., 2014. European centre for ecotoxicology and toxicology of chemicals. In: Encyclopedia of toxicology. Elsevier, pp. 547–548. https://doi.org/10.1016/B978-0-12-386454-3.00505-4.
[13] Chamas, A., Moon, H., Zheng, J., Qiu, Y., Tabassum, T., Jang, J.H., et al., 2020. Degradation rates of plastics in the environment. ACS Sustain Chem Eng 8, 3494–3511. https://doi.org/10.1021/acssuschemeng.9b06635.
[14] Che, K., Lyu, P., Wan, F., Ma, M., 2019. Investigations on aging behavior and mechanism of polyurea coating in marine atmosphere. Materials 12, 3636. https://doi.org/10.3390/ma12213636.
[15] Chen, C., Chen, L., Yao, Y., Artigas, F., Huang, Q., Zhang, W., 2019. Organotin release from polyvinyl chloride microplastics and concurrent photodegradation in water: impacts from salinity, dissolved organic matter, and light exposure. Environ Sci Technol 53, 10741–10752. https://doi.org/10.1021/acs.est.9b03428.
[16] Chen, Y., Gao, B., Yang, Y., Pan, Z., Liu, J., Sun, K., et al., 2022. Tracking microplastics biodegradation through CO2 emission: Role of photoaging and mineral addition. J Hazard Mater 439, 129615. https://doi.org/10.1016/j.jhazmat.2022.129615.
[17] Ciani, A., Goss, K. -U., Schwarzenbach, R.P., 2005. Light penetration in soil and particulate minerals. Eur J Soil Sci 56, 561–574. https://doi.org/10.1111/j.1365-2389.2005.00688.x.
[18] Cox, C., Surgan, M., 2006. Unidentified inert ingredients in pesticides: implications for human and environmental health. Environ Health Perspect 114, 1803–1806. https://doi.org/10.1289/ehp.9374.
[19] Ding, L., Yu, X., Guo, X., Zhang, Y., Ouyang, Z., Liu, P., et al., 2022. The photodegradation processes and mechanisms of polyvinyl chloride and polyethylene terephthalate microplastic in aquatic environments: important role of clay minerals. Water Res 208, 117879. https://doi.org/10.1016/j.watres.2021.117879.
[20] Du, J., Ibaseta, N., Guichardon, P., 2022. Characterization of polyurea microcapsules synthesized with an isocyanate of low toxicity and eco-friendly esters via microfluidics: shape, shell thickness, morphology and encapsulation efficiency. Chem Eng Res Des 182, 256–272. https://doi.org/10.1016/j.cherd.2022.03.026.
[21] Duan, J., Li, Y., Gao, J., Cao, R., Shang, E., Zhang, W., 2022. ROS-mediated photoaging pathways of nano- and micro-plastic particles under UV irradiation. Water Res 216, 118320. https://doi.org/10.1016/j.watres.2022.118320.
[22] ECHA, E.C.A., 2019. Annex XV restriction report – microplastics, proposal for restriction of intentionally added microplastics.
[23] European Commission. ANNEX to the Commission Regulation (EU) amending Annex XVII to Regulation (EC) No 1907/2006 of the European Parliament and of the Council concerning the Registration, Evaluation, Authorisation and Restriction of Chemicals (REACH) as regards synthetic polymer microparticles; 2023.
[24] European Food Safety Authority, 2014. EFSA guidance document for evaluating laboratory and field dissipation studies to obtain DegT50 values of active substances of plant protection products and transformation products of these active substances in soil. In: EFS2, 12. https://doi.org/10.2903/j.efsa.2014.3662.
[25] European Food Safety Authority (EFSA), Egsmose, M., Fait, G., Janzen, W., Jentzsch, F., Lava, R., et al., 2022. Scientific guidance on soil phototransformation products in groundwater – consideration, parameterisation and simulation in the exposure assessment of plant protection products. EFS2 20. https://doi.org/10.2903/j.efsa.2022.7119.
[26] FAO, F and AO of the UN. Assessment of agricultural plastics and their sustainability: a call for action. Rome, Italy; 2021.
[27] Feldman, D., 2002. Polymer weathering: photo-oxidation. J Polym Environ 10, 163–173. https://doi.org/10.1023/A:1021148205366.
[28] Gewert, B., Plassmann, M.M., MacLeod, M., 2015. Pathways for degradation of plastic polymers floating in the marine environment. Environ Sci Process Impacts 17, 1513–1521. https://doi.org/10.1039/C5EM00207A.
[29] Grause, G., Chien, M.-F., Inoue, C., 2020. Changes during the weathering of polyolefins. Polym Degrad Stab 181, 109364. https://doi.org/10.1016/j.polymdegradstab.2020.109364.
[30] Gulmine, J.V., Janissek, P.R., Heise, H.M., Akcelrud, L., 2003. Degradation profile of polyethylene after artificial accelerated weathering. Polym Degrad Stab 79, 385–397. https://doi.org/10.1016/S0141-3910(02)00338-5.
[31] Hahn, S., Hennecke, D., 2023. What can we learn from biodegradation of natural polymers for regulation? Environ Sci Eur 35, 50. https://doi.org/10.1186/s12302-023-00755-y.
[32] Haider, T.P., Völker, C., Kramm, J., Landfester, K., Wurm, F.R., 2019. Plastics of the future? The impact of biodegradable polymers on the environment and on society. Angew Chem Int Ed 58, 50–62. https://doi.org/10.1002/anie.201805766.
[33] Hamid, S., 2000. Handbook of polymer degradation. Marcel Dekker.
[34] Hann, S., Fletcher, E., Sherrington, C., Molteno, S., Elliott, L., 2021. Conventional and biodegradable plastics in agriculture. Report for DG environment of the European Commission.
[35] Hassink, J., Buda, J., Multsch, S., Nellen, S., Noe, S., Schmidt, T., 2024. Development of a new test design to investigate the degradation of pesticides in soil under sunlight conditions. Environ Sci Eur 36, 151. https://doi.org/10.1186/s12302-024-00974-x.
[36] Jansen, M.A.K., Andrady, A.L., Bornman, J.F., Aucamp, P.J., Bais, A.F., Banaszak, A.T., et al., 2024. Plastics in the environment in the context of UV radiation, climate change and the Montreal protocol: UNEP environmental effects assessment panel, update 2023. Photochem Photobiol Sci 23, 629–650. https://doi.org/10.1007/s43630-024-00552-3.
[37] Karagianni, K., Kuntzmann-Dembele, F., Bocokic, V., Charbonnier, A., Harrison, I., Kreutzer, G., et al., 2024. Fragrance encapsulates: effect of polymeric shell purification method on the accuracy of biodegradability testing. Environ Toxic Chem 43, 1242–1249. https://doi.org/10.1002/etc.5852.
[38] Kookana, R.S., Boxall, A.B.A., Reeves, P.T., Ashauer, R., Beulke, S., Chaudhry, Q., et al., 2014. Nanopesticides: guiding principles for regulatory evaluation of environmental risks. J Agric Food Chem 62, 4227–4240. https://doi.org/10.1021/jf500232f.
[39] Krause, J., Egger, H., 2021. Aqueous capsule suspension concentrates based on polyurea shell material containing polyfunctional aminocarboxylic esters [WO2021136758].
[40] La Mantia, F.P., 1986. Influence of processing conditions on the photo-oxidation of polypropylene films. Polym Degrad Stab 15, 283–290.
[41] Lemaire, J., Arnaud, R., Lacoste, J., 1988. The prediction of the long-term photoageing of solid polymers. Acta Polym 39, 27–32. https://doi.org/10.1002/actp.1988.010390106.
[42] Liu, P., Wu, X., Peng, J., Wang, H., Shi, Y., Huang, H., et al., 2021. Critical effect of iron red pigment on photoaging behavior of polypropylene microplastics in artificial seawater. J Hazard Mater 404, 124209. https://doi.org/10.1016/j.jhazmat.2020.124209.
[43] Lucas, N., Bienaime, C., Belloy, C., Queneudec, M., Silvestre, F., Nava-Saucedo, J.-E., 2008. Polymer biodegradation: mechanisms and estimation techniques – a review. Chemosphere 73, 429–442. https://doi.org/10.1016/j.chemosphere.2008.06.064.
[44] Mao, R., Lang, M., Yu, X., Wu, R., Yang, X., Guo, X., 2020. Aging mechanism of microplastics with UV irradiation and its effects on the adsorption of heavy metals. J Hazard Mater 393, 122515. https://doi.org/10.1016/j.jhazmat.2020.122515.
[45] McNeill, K., Canonica, S., 2016. Triplet state dissolved organic matter in aquatic photochemistry: reaction mechanisms, substrate scope, and photophysical properties. Environ Sci Process Impacts 18, 1381–1399. https://doi.org/10.1039/C6EM00408C.
[46] Mekaru, H., 2020. Effect of agitation method on the nanosized degradation of polystyrene microplastics dispersed in water. ACS Omega 5, 3218–3227. https://doi.org/10.1021/acsomega.9b03278.
[47] Mitrano, D.M., Wohlleben, W., 2020. Microplastic regulation should be more precise to incentivize both innovation and environmental safety. Nat Commun 11, 5324. https://doi.org/10.1038/s41467-020-19069-1.
[48] Nederstigt, T.A.P., Brinkmann, B.W., Peijnenburg, W.J.G.M., Vijver, M.G., 2024. Sustainability claims of nanoenabled pesticides require a more thorough evaluation. Environ Sci Technol 58, 2163–2165. https://doi.org/10.1021/acs.est.3c10207.
[49] OECD Draft TG (Ed.), 2002. Draft TG – proposal for a new guideline: phototransformation of chemicals on soil surface. OECD Publishing, Paris.
[50] OECD TG 301 (Ed.), 1992. Test No. 301: ready biodegradability, OECD guidelines for the testing of chemicals, section 3. OECD Publishing, Paris. https://doi.org/10.1787/9789264070349-en.
[51] OECD TG 307 (Ed.), 2002. Test no. 307: aerobic and anaerobic transformation in soil, OECD guidelines for the testing of chemicals, section 3. OECD Publishing, Paris. https://doi.org/10.1787/9789264070509-en.
[52] OECD TG 316 (Ed.), 2008. Test no. 316: phototransformation of chemicals in water direct photolysis, OECD guidelines for the testing of chemicals, section 3. OECD Publishing, Paris. https://doi.org/10.1787/9789264067585-en.
[53] Pfohl, P., Santizo, K., Sipe, J., Wiesner, M., Harrison, S., Svendsen, C., et al., 2025. Environmental degradation and fragmentation of microplastics: dependence on polymer type, humidity, UV dose and temperature. Microplast Nanoplast 5, 7. https://doi.org/10.1186/s43591-025-00118-9.
[54] Quijada, R., Narváez, A., Rojas, R., Rabagliati, F.M., Barrera Galland, G., Santos Mauler, R., Benavente, R., Pérez, E., Pereña, J.M., Bello, A., 1999. Synthesis and characterization of copolymers of ethylene and 1-octadecene using the rac-Et (Ind)2ZrCl2/MAO catalyst system. Macromol Chem Phys 200, 1306–1310.
[55] Rabek, J.F., Rånby, B., 1974. Studies on the photooxidation mechanism of polymers. II. The role of quinones as sensitizers in the photooxidative degradation of polystyrene. J Polym Sci Polym Chem Ed 12, 295–306. https://doi.org/10.1002/pol.1974.170120204.
[56] Rajakumar, K., Sarasvathy, V., Thamarai Chelvan, A., Chitra, R., Vijayakumar, C. T., 2009. Natural weathering studies of polypropylene. J Polym Environ 17, 191–202. https://doi.org/10.1007/s10924-009-0138-7.
[57] Rose, R.-S., Richardson, K.H., Latvanen, E.J., Hanson, C.A., Resmini, M., Sanders, I. A., 2020. Microbial degradation of plastic in aqueous solutions demonstrated by CO2 evolution and quantification. IJMS 21, 1176. https://doi.org/10.3390/ijms21041176.
[58] Sander, M., Weber, M., Lott, C., Zumstein, M., Künkel, A., Battagliarin, G., 2023. Polymer biodegradability 2.0: a holistic view on polymer biodegradation in natural and engineered environments. In: Künkel, A., Battagliarin, G., Winnacker, M., Rieger, B., Coates, G. (Eds.), Synthetic biodegradable and biobased polymers, advances in polymer science. Springer International Publishing, Cham, pp. 65–110. https://doi.org/10.1007/12_2023_163.
[59] Schnabel, W., 1981. Polymer degradation: principles and practice, 2. Carl Hanser Verlag, Wien, p. 133.

[60] Si, T., Kim, H.Y., Oh, K., 2021. One-pot direct oxidation of primary amines to carboxylic acids through tandem *ortho* -naphthoquinone-catalyzed and TBHP-promoted oxidation sequence. Chem A Eur J 27, 18150–18155. https://doi.org/10.1002/chem.202103450.

[61] Silva, A.B., Bastos, A.S., Justino, C.I.L., Da Costa, J.P., Duarte, A.C., Rocha-Santos, T.A.P., 2018. Microplastics in the environment: challenges in analytical chemistry – a review. Anal Chim Acta 1017, 1–19. https://doi.org/10.1016/j.aca.2018.02.043.

[62] Sinn, H., Kaminsky, W., Vollmer, H., Woldt, R., 1980. Living Polymers" on Polymerization with Extremely Productive Ziegler Catalysts. Angew Chem Int Engl 19, 390–392. https://doi.org/10.1002/anie.198003901.

[63] Tantawi, O., Joo, W., Martin, E.E., Av-Ron, S.H.M., Bannister, K.R., Prather, K.L.J., et al., 2025. Designing for degradation: the importance of considering biotic and abiotic polymer degradation. Environ Sci Process Impacts 27, 1303–1316. https://doi.org/10.1039/D5EM00079C.

[64] Teggers, E.-M., Hardebusch, J., Meisterjahn, B., Simon, M., Hennecke, D., Heumann, R., et al., 2025. Diversifying endpoints in biodegradation testing of microplastics. Environ Sci Eur 37, 65. https://doi.org/10.1186/s12302-025-01096-8.

[65] Teggers, E.-M., Heck, S., Meisterjahn, B., Simon, M., Hennecke, D., Heumann, R., et al., 2025. Modified oil extraction of pristine and weathered synthetic polyurea microcapsules and polyethylene microplastics from soil. Microplast Nanoplast. https://doi.org/10.1186/s43591-025-00121-0.

[66] Tester, M., Morris, C., 1987. The penetration of light through soil. Plant Cell Environ 10, 281–286. https://doi.org/10.1111/j.1365-3040.1987.tb01607.x.

[67] Tidjani, A., Arnaud, R., 1993. Photo-oxidation of linear low density polyethylene: a comparison of photoproducts formation under natural and accelerated exposure. Polym Degrad Stab 39, 285–292. https://doi.org/10.1016/0141-3910(93)90003-2.

[68] UNEP. Resolution adopted by the United Nations Environment Assembly on 2 March 2022. 5/5. Nature-based solutions for supporting sustainable development; 2022.

[69] Wang, J., Chen, J., Qiao, X., Zhang, Y., Uddin, M., Guo, Z., 2019. Disparate effects of DOM extracted from coastal seawaters and freshwaters on photodegradation of 2,4-dihydroxybenzophenone. Water Res 151, 280–287. https://doi.org/10.1016/j.watres.2018.12.045.

[70] Washington, J.W., Jenkins, T.M., Rankin, K., Naile, J.E., 2015. Decades-scale degradation of commercial, side-chain, fluorotelomer-based polymers in soils and water. Environ Sci Technol 49, 915–923. https://doi.org/10.1021/es504347u.

[71] Wu, X., Liu, P., Gong, Z., Wang, H., Huang, H., Shi, Y., et al., 2021. Humic acid and fulvic acid hinder long-term weathering of microplastics in lake water. Environ Sci Technol 55, 15810–15820. https://doi.org/10.1021/acs.est.1c04501.

[72] Wu, X., Liu, P., Wang, H., Huang, H., Shi, Y., Yang, C., et al., 2021. Photo aging of polypropylene microplastics in estuary water and coastal seawater: Important role of chlorine ion. Water Res 202, 117396. https://doi.org/10.1016/j.watres.2021.117396.

[73] Xu, Y., Ou, Q., Van Der Hoek, J.P., Liu, G., Lompe, K.M., 2024. Photo-oxidation of micro- and nanoplastics: physical, chemical, and biological effects in environments. Environ Sci Technol 58, 991–1009. https://doi.org/10.1021/acs.est.3c07035.

[74] Yu, X., Xu, Y., Lang, M., Huang, D., Guo, X., Zhu, L., 2022. New insights on metal ions accelerating the aging behavior of polystyrene microplastics: effects of different excess reactive oxygen species. Sci Total Environ 821, 153457. https://doi.org/10.1016/j.scitotenv.2022.153457.

[75] Zhang, Y., Cheng, F., Zhang, T., Li, C., Qu, J., Chen, J., et al., 2022. Dissolved organic matter enhanced the aggregation and oxidation of nanoplastics under simulated sunlight irradiation in water. Environ Sci Technol 56, 3085–3095. https://doi.org/10.1021/acs.est.1c07129.

[76] Zhang, S., Li, Y., Jiang, L., Cao, M., Xing, Z., Dong, D., et al., 2025. Insights on the characteristics of plastic surface degradation and biofilm microorganisms: exploring the impacts of three aerobic composting (AC) as well as UV irradiation and cycles of freeze-thaw (CFTs). J Hazard Mater 495, 138960. https://doi.org/10.1016/j.jhazmat.2025.138960.

[77] Zhu, K., Sun, Y., Jiang, W., Zhang, C., Dai, Y., Liu, Z., et al., 2022. Inorganic anions influenced the photoaging kinetics and mechanism of polystyrene microplastic under the simulated sunlight: role of reactive radical species. Water Res 216, 118294. https://doi.org/10.1016/j.watres.2022.118294.